

Short communication

Photolysis of diruthenium hexacarbonyl tetrahedrane compounds in Nujol glass matrices

Thomas E. Bitterwolf^{a,*}, Javier A. Cabeza^b

^a Department of Chemistry, University of Idaho, Moscow, ID 83844-2343, USA

^b Departamento de Química Orgánica e Inorgánica, Instituto de Química Organometálica Enrique Moles, Universidad de Oviedo-CSIC, E-33071 Oviedo, Spain

Received 19 November 2002; accepted 25 November 2003

Available online 29 July 2004

Abstract

The photochemistry of five diruthenium hexacarbonyl tetrahedrane compounds, $\text{Ru}_2(\text{CO})_6(\mu\text{-S}_2\text{C}_6\text{H}_4)$ (**1**), $\text{Ru}_2(\text{CO})_6(\mu\text{-S}_2\text{C}_2\text{H}_4)$ (**2**), $\text{Ru}_2(\text{CO})_6(\mu\text{-S}_2\text{C}_3\text{H}_6)$ (**3**), $\text{Ru}_2(\text{CO})_6(\mu\text{-SCH}_2\text{CH}_3)_2$ (**4**), and $\text{Ru}_2(\text{CO})_6(\mu\text{-dmpz})_2$ (**5**), where $\text{dmpz} = 3,5\text{-dimethylpyrazolate}$, have been examined in frozen Nujol glasses at ca. 90 K. Compounds **1–4** are found to lose CO upon UV photolysis to form two isomeric photoproducts, while **5** is found to form one product almost exclusively. The various photoproducts are assigned to axial and equatorial CO-loss species on the basis of the spectra of analogous triphenylphosphine pentacarbonyl derivatives.
© 2004 Published by Elsevier B.V.

Keywords: Ruthenium; Diruthenium hexacarbonyls; Photochemistry; Photochemical reactions; Tetrahedrane compounds

1. Introduction

For some time we have been interested in the photochemistry of dimetalla hexacarbonyl tetrahedrane complexes where a variety of groups may form the two non-metallic vertices of the tetrahedron. These compounds are characterized by a bent metal–metal bond with both metals in a pseudo-octahedral geometry. Carbonyl ligands are oriented equatorial (*cis*) or axial (*trans*) relative to the metal–metal bond. In the case of the $\text{Co}_2(\text{CO})_6(\text{alkyne})$ series, observations in our laboratory [1] and that of Gordon et al. [2] indicate that photolysis results in loss of a carbonyl ligand to give rise to one of the two possible isomeric pentacarbonyl species. We found that this species rearranged to a second pentacarbonyl isomer either thermally or photochemically.

A small number of diruthenium hexacarbonyl tetrahedrane compounds have been reported and in the

current work we shall describe the photochemistry of compounds **1–5**, Table 1. As shall be described below, the photochemistry of these compounds is reminiscent of that of the dicobalt hexacarbonyl alkyne series.

2. Results and discussion

Compounds **1** [3] and **5** [4] were prepared as described by Cabeza et al. Compounds **2**, **3**, and **4** were also prepared in low yields (3%, 10%, and 33%, respectively) by this route and were found to be spectroscopically identical to these compounds prepared by reaction of the respective dithiols with $\text{Ru}_3(\text{CO})_{12}$ [5].

In the papers describing the synthesis of Compound **4**, this complex was only characterized by its IR spectrum [5c,5d]. In our hands, column chromatography of the reaction mixture established the presence of two isomers (8:1 ratio by integration) which were very difficult to completely separate. NMR spectra revealed that the major isomer possesses two distinct ethyl group environments while the ethyl groups of the minor isomer have identical environments. By analogy with the iron derivatives, $\text{Fe}_2(\text{CO})_6(\mu\text{-SR})_2$, [6] we assign the major

* Corresponding author. Tel.: +1-208-885-6361; fax: +1-208-885-6173.

E-mail address: bitterte@uidaho.edu (T.E. Bitterwolf).

Table 1
Infrared spectra (cm⁻¹) of **1–5** and their CO-loss photoproducts

Compound	Initial spectrum	Equatorial CO-loss	Axial CO-loss
Ru ₂ (CO) ₆ (S ₂ C ₆ H ₄) (1)	2090 m	2087	2068
	2062 s	2018	2019
	2012 s (broad)	1949	2000
			1987
			1962
Ru ₂ (CO) ₆ (S ₂ C ₂ H ₄) (2)	2087 m	2084	2063
	2056 s	2015	2026
	2011 s	1949	2016
	2004 s		1987
	1993 m		1954
Ru ₂ (CO) ₆ (S ₂ C ₃ H ₆) (3)	2086 m	2082	2064
	2055 s	1948	2014
	2009 s		1995
	2002 s		1986
	1992 m		1952
Ru ₂ (CO) ₆ (SC ₂ H ₅) ₂ (4) (e, a isomer) ¹	2082 m	2080	2011
	2053 s	1939	1989
	2007 s		1877
	1997 s		1948
Ru ₂ (CO) ₆ (dmpz) ₂ (5)	2089 m	2097	
	2056 s	2030	
	2011 s (broad)	2017	
	1996 m	2002	
		1941z	

Photoproduct bands are only listed where they have been firmly established by back-photolysis or annealing experiments.

¹ Only the highest energy band of the photoproduct of the e, e isomer of **4** could be observed at 2121 cm⁻¹.

isomer to a species in which one ethyl group is in an axial orientation while the second is in an equatorial orientation (e, a isomer), Fig. 1. Steric considerations suggest that the minor isomer is probably one in which both ethyl groups are in equatorial orientations (e, e isomer), Fig. 1. Curiously, the resonances of the axial ethyl group in the e, a isomer are shifted upfield relative to those of the equatorial ethyl group suggesting a strong magnetic anisotropy. At room temperature no carbonyl resonances could be observed for **4**, but all three symmetry-predicted resonances were observed at -30 °C indicating that these carbonyls are fluxional.

Compounds **1–5** are pale yellow crystalline solids. Electronic spectra of the compounds are very similar. Compounds **1–4** have absorption maxima between 324 and 340 nm and molar absorptivity values between 3800 and 4800. Compound **5** has an absorption maximum at 303 nm and a molar absorptivity of 10,000. The yellow color in each case results from the tail of the band at about 330 nm that extends into the visible.

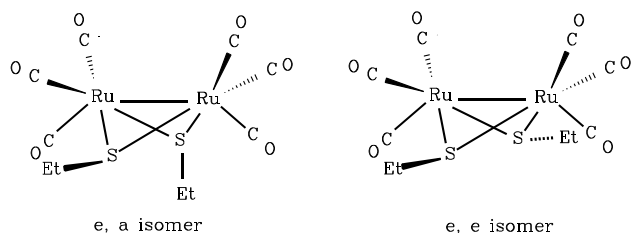


Fig. 1. e, a and e, e isomers of **4**.

Nujol solutions of the ruthenium compounds were frozen to ca. 90 K as previously described [7]. Photolysis of **1–4** in the visible region resulted in no significant changes in the IR spectra of the compounds. UV photolysis, 330 nm < λ_{max} < 400 nm, gave rise in each case to a bleaching of the bands of the starting material and appearance of as many as seven new carbonyl bands in addition to a band at ca. 2131 cm⁻¹ attributable to free CO in the Nujol matrix. Fig. 2 illustrates the spectral changes that are observed for **1** upon photolysis. Spectra of compounds **2–4** are similar in appearance. In the case of **4** both isomers were observed to be photolyzed, but only the highest frequency band in the product spectrum

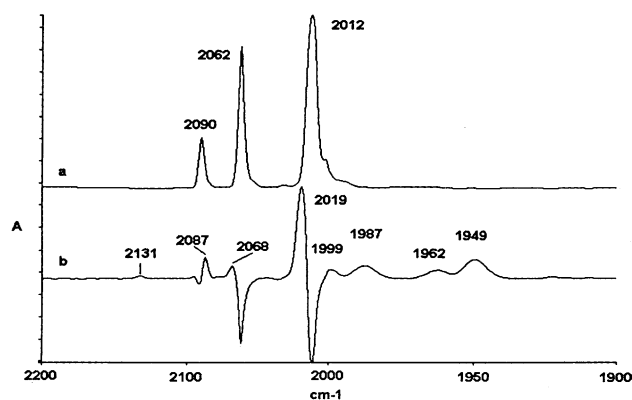


Fig. 2. (a) Spectrum of **1** in frozen Nujol before photolysis. (b) Difference spectrum after 10 min photolysis (330 nm < λ_{irr} < 400 nm).

of the minor isomer could be assigned with confidence. IR spectral data are presented in Table 1. Subsequent back-photolysis of these samples at long wavelength, typically $\lambda_{\text{max}} = 500 \pm 70$ nm, resulted in the bleaching of some of the photoproduct bands and the growth of the remaining bands. In each case some starting material was also formed during back-photolysis. The resulting difference spectra permit clear assignment of the bands of one of the photoproducts and partial assignment of the bands of the second photoproduct. Overlap of the two product spectra and the starting material spectra make a complete assignment of the bands of the second photoproduct impossible. In the case of **2**, annealing the back-photolyzed sample to ca. 160 K followed by refreezing to ca. 90 K allowed an additional band to be identified.

Unlike **1–4**, photolysis of **5** at wavelengths as long as 500 nm was observed to initiate photochemistry. Photolysis of **5** resulted in a very much simpler product spectrum, Fig. 3, in which five metal carbonyl bands are observed in addition to the band at 2131 cm^{-1} , associated with free CO. The photochemical reactivity of **5** at 500 nm may well arise from the higher molar absorptivity of the 303 nm electronic absorption band relative to the molar absorptivities of **1–4**. The doubling of the molar absorptivity upon replacement of sulfide bridges by dimethylpyrazolate may result from an overlap of the electronic transitions of the aromatic pyrazolate ring with those of the Ru–Ru bond.

Photolysis of these diruthenium hexacarbonyl tetrahedrane compounds give rise to two, isomeric CO-loss species. One species, A, is characterized by a high energy carbonyl stretching band above or just slightly below the highest energy carbonyl band of the starting material and a second very low energy carbonyl band between 1940 and 1950 cm^{-1} . This lower band is still well within the region typically associated with a terminal carbonyl group. Mid-energy bands for this species are obscured for **3** and **4**, but other bands between 2000 and 2040 cm^{-1} are observed for **1**, **2** and **5**.

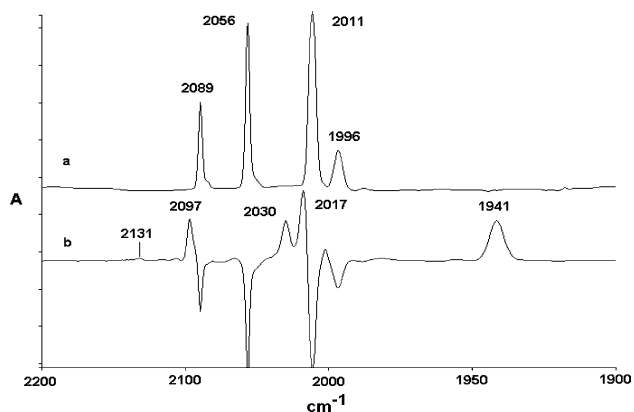
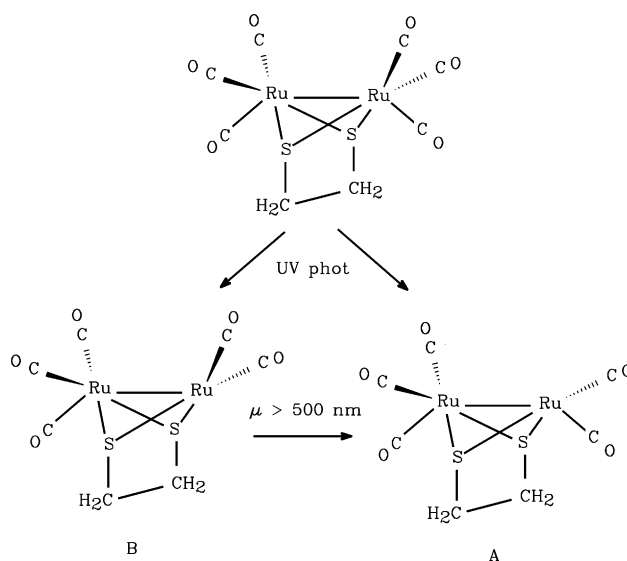


Fig. 3. (a) Spectrum of **5** in frozen Nujol before photolysis. (b) Difference spectrum after 30 min photolysis ($330 \text{ nm} < \lambda_{\text{irr}} < 400 \text{ nm}$).

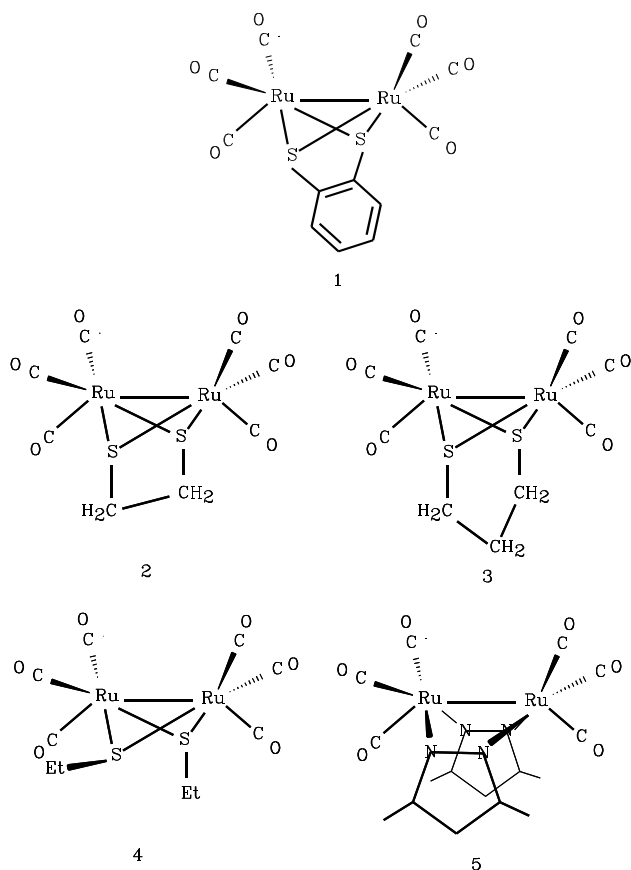
The second photoproduct, B, is characterized by a high energy band at about 2065 cm^{-1} and additional bands about 2020, 1990 and 1960 cm^{-1} . Photoproducts A and B appear to be generated together in the UV, but subsequent long wavelength photolysis converts B to A.

Loss of an axial carbon monoxide ligand from a dimetalla hexacarbonyl tetrahedrane molecule gives rise to a pentacarbonyl fragment with C_s mirror symmetry, while loss of an equatorial carbonyl gives rise to a fragment with C_1 symmetry. Both fragments are predicted to have five carbonyl IR bands, so simple symmetry arguments do not allow us to differentiate between the two possible structures.

To assign the structures of these fragments we note that compound **5** is known to undergo substitution by either PPh_3 or PCy_3 to yield exclusively the equatorial isomer [4a]. The analogous $\text{P}(\text{C}_6\text{H}_5)_3$ derivatives of compounds **1–3** are known to be axially substituted [3a,4a]. Thus, the IR spectrum of $\text{Ru}_2(\text{CO})_5(\text{PPh}_3)(\mu\text{-dmpz})_2$ has a high energy carbonyl band at 2088 cm^{-1} , just one wavenumber below that of **5**, while the PPh_3 derivatives of **1–3** have a high energy band at about 2060 cm^{-1} . While it may be somewhat bold to assert that a weakly π -bonding PPh_3 ligand will produce spectral effects analogous to those observed in a photoproduct in which a solvent (Nujol) molecule occupies the binding site, the striking similarity in stretching frequencies appears to support this claim. On this basis, we assign the photofragments with their highest carbonyl stretching frequency about 2090 cm^{-1} to equatorial CO-loss and those with their highest carbonyl stretching frequency at about 2065 cm^{-1} to axial CO-loss. The observed back-photolysis may now be interpreted as a conversion of the equatorial isomer to an axial isomer. This is summarized for compound **2** in Scheme 1.



Scheme 1. Summary of photolysis species for **2**. Compound **5** only appears to generate the equatorial CO-loss species A.



A question that remains unanswered for these compounds is the nature of the electronic transition that manifests itself in the rupture of a metal–CO bond. Fensky and coworkers [8] have examined the bonding in $\text{Fe}_2(\text{CO})_6\text{B}_2$ compounds using parameter-free molecular orbital calculations and have established that the HOMO and LUMO orbitals are, for the most part, metal based orbitals. The HOMO is the well known “bent” bond, while the LUMO is predominantly the antibonding orbital of this bent bond. Orbitals derived from DFT calculations of **2**, Figs. 4 and 5, indicate that the bonding in the ruthenium compound parallels that of the iron series in that the HOMO is characterized by a Ru–Ru bond with some back-bonding character to the equatorial carbonyls. Interestingly, there is an antibonding component to this orbital between the metal and the axial carbonyl groups. The LUMO is found to be strongly antibonding between the metals. Analogous

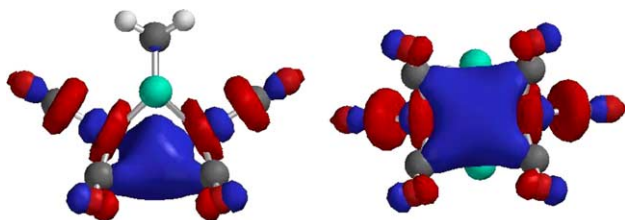


Fig. 4. HOMO Orbital of **2** from DFT calculations.

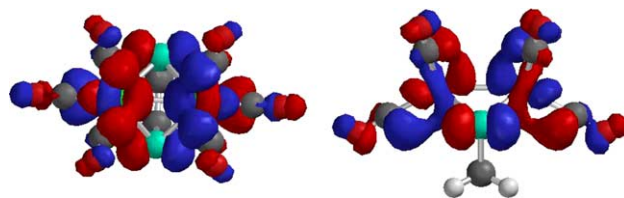


Fig. 5. LUMO orbital of **2** from DFT calculations.

information has been obtained from EHMO calculations on complex **1** [3b].

The theoretical models suggest that the lowest energy electronic excitation would be expected to be a $\sigma \rightarrow \sigma^*$ transition, resulting in rupture of the metal–metal bond. The molar absorptivity for the excitation that appears to be responsible for CO loss is in excess of 10^4 thus this is clearly an allowed transition. It is possible that there might be intersystem crossing leading to a triplet excited state and that CO loss occurs from such a triplet. Alternately, CO-loss may compete with energy transfer to solvent from the vibrationally hot species arising from the absorption of a 330 nm photon.

As we shall report elsewhere, the simplicity of the diruthenium hexacarbonyl tetrahedrane compounds stands in contrast to the analogous iron compounds for which a bridging carbonyl isomer is observed in several cases. These studies are relevant to the broader question of the photochemistry of dimetalla tetrahedrane compounds, such as those that form the active site of the iron-only hydrogenase enzymes.

3. Experimental

Experimental procedures for the photochemical study of samples in frozen Nujol glass matrices have been previously reported [7]. DFT calculations were carried out using Spartan Pro V 1.0.1 and employing the pBP86/DN* basis set.

Compounds **1** [3] and **5** [4a] were prepared by reaction of **1**, 2-benzene dithiol or 2, 4-dimethylpyrazole, respectively, with the pale yellow, $[\text{Ru}(\text{CO})_2\text{Cl}_2]$, intermediate formed by reaction of $\text{RuCl}_3 \cdot n\text{H}_2\text{O}$ with CO in refluxing 2-methoxyethanol as described by Cabeza et al. [5]. Compounds **2**, **3**, and **4** were also prepared in low yield (3%, 10%, and 33%, respectively) by the same route as **1** and **5** and were found to be spectrally identical to these compounds prepared by reaction of the respective dithiols with $\text{Ru}_3(\text{CO})_{12}$.

Chromatography of **4** on a $40 \text{ cm} \times 1 \text{ cm}$ column of alumina with hexane as the eluant gave two products (IR identification). Early cuts of the yellow band indicated that one isomer, subsequently shown to be the axial, equatorial (a, e) isomer, was recovered, but subsequent cuts were shown to contain increasing amounts of a second isomer, believed to be the equatorial,

equatorial (e, e) isomer. The ratio in the bulk recovered material was about 8:1. ^1H , ^{13}C , and 2D NMR methods were used to characterize and assign all resonances except for the metal carbonyl resonances. Major, a, e isomer. IR (petroleum ether): 2082 m, 2053 s, 2007 s, 1997 s cm^{-1} . ^1H NMR (CDCl_3): 2.59 (e- CH_2 , q, $J = 7.4$ Hz), 2.23 (a- CH_2 , q, $J = 7.3$ Hz), 1.39 (e- CH_3 , t, $J = 7.4$), 1.10 (a- CH_3 , t, $J = 7.3$ Hz). ^{13}C NMR (CDCl_3): 197.4 (Ru-CO), 195.7 (Ru-CO), 189.4 (Ru-CO), 34.4 (e- CH_2), 19.0 (a- CH_2), 18.6 (e- CH_3), 18.4 (a- CH_3). Minor, e, e isomer. IR (petroleum ether): 2115 w, 2064 m, 2024 m (additional bands may be obscured by the major isomer). ^1H NMR (CDCl_3): 2.28 (e- CH_2 , q, $J = 7.3$ Hz), 1.31 (e- CH_3 , t, $J = 7.3$ Hz). ^{13}C NMR (CDCl_3): (Ru-CO resonances not observed), 33.7 (e- CH_2), 18.8 (e- CH_3). Mass spectrometry of an 8:1 sample (EI): 492 (95%, M^+), 464 (59%, M^+-28), 436 (60%, $\text{M}^+-2 \times 28$), 408 (66%, 3×28), 380 (81%, $\text{M}^+-4 \times 28$), 352 (36%, $\text{M}^+-5 \times 28$), 324 (39%, $\text{M}^+-6 \times 28$), 296 (44%, $\text{M}^+-7 \times 28$), 268 (68%, $\text{M}^+-8 \times 28$). Note: ^{101}Ru mass peak was used as the reference. CO and C_2H_4 have identical masses thus it is not possible to identify fragment peaks as M-CO or M- C_2H_4 .

Acknowledgements

We thank the Research Corporation for a Research Opportunity grant (to T.E.B.).

References

- [1] T.E. Bitterwolf, W.B. Scallorn, C.A. Weiss, J. Organomet. Chem. 605 (2000) 7–14.
- [2] C.M. Gordon, M. Kiszka, I.R. Dunkin, W.J. Kerr, J.S. Scott, J. Gebicki, J. Organomet. Chem. 554 (1998) 147–154.
- [3] (a) J.A. Cabeza, M.A. Martinez-Garcia, V. Riera, D. Ardura, S. Garcia-Granda, J.F. Vander Maelen, Eur. J. Inorg. Chem. (1999) 1133–1139; (b) J.A. Cabeza, M.A. Martines-Garcia, V. Riera, D. Ardura, S. Garcia-Granda, Organometallics 17 (1998) 1471–1477.
- [4] (a) J.A. Cabeza, C. Landázuri, L.A. Oro, D. Belletti, A. Tiripicchio, M. Tiripicchio-Camellini, J. Chem. Soc., Dalton Trans. (1989) 1093–1100; (b) J.A. Cabeza, C. Landázuri, L.A. Oro, A. Tiripicchio, M. Tiripicchio-Camellini, J. Organomet. Chem. 322 (1987) C16–C20; (c) J.A. Cabeza, L.A. Oro, Inorg. Synth. 31 (1997) 217–220.
- [5] (a) K.M. Hanif, S.E. Kabir, M.A. Mottalib, M.B. Hursthouse, K.M.A. Malik, E. Rosenberg, Polyhedron 19 (2000) 1073–1080; (b) R.D. Adams, J.H. Yamamoto, Organometallics 14 (1995) 3704–3711; R.D. Adams, L. Chen, J.H. Yamamoto, Inorg. Chim. Acta 229 (1995) 47–54; (c) B.F.G. Johnson, R.D. Johnston, P.L. Josty, J. Lewis, I.G. Williams, Nature (1967) 901–902; (d) G. Cetini, O. Gambino, E. Sappa, M. Valle, J. Organomet. Chem. 15 (1968) P4–P6.
- [6] D. Seyferth, R.S. Henderson, L.-C. Song, Organometallics 1 (1982) 125–133, and references therein.
- [7] T.E. Bitterwolf, W.B. Scallorn, J.T. Bays, C.A. Weiss, J.C. Linehan, J. Franz, R. Poli, J. Organomet. Chem. 652 (2002) 95–104.
- [8] B.K. Teo, M.B. Hall, R.F. Fensky, L.F. Dahl, Inorg. Chem. 14 (1975) 3103–3117.